EuTe. II. Resistivity and Hall Effect

Y. Shapira, S. Foner, and N. F. Oliveira, Jr. *†
Francis Bitter National Magnet Laboratory,‡ Massachusetts Institute of Technology, Cambridge, Massachusetts 02139

and

T. B. Reed
Lincoln Laboratory, § Massachusetts Institute of Technology, Lexington, Massachusetts 02173
(Received 7 June 1971)

The resistivity and Hall effect in n-type EuTe single crystals containing $\sim 10^{19}$ carriers/cm^3 were studied at $1.6 < T < 300$ K in magnetic fields up to 140 kOe. At temperatures $T \lesssim 2T_N$, where $T_N \cong 9.7$ K is the Néel temperature, the resistivity ρ at $H = 0$ increased rapidly with decreasing T. This increase in ρ was removed entirely by the application of a high magnetic field H. At 14.5 K, ρ decreased gradually with increasing H. Hall measurements showed that the negative magnetoresistance at 14.5 K was due almost entirely to an increase in the mobility, and not to an increase in the number of charge carriers. At liquid-helium temperatures, $\rho(H)$ exhibited different behaviors in three different ranges of the field H: (i) At $0 \leq H \lesssim 10^3$ Oe, ρ decreased very rapidly with H, with the result that ρ (1 kOe) was at least one order of magnitude smaller than $\rho(0)$; (ii) in the canted phase ($1 \lesssim H \lesssim 70$ kOe), ρ decreased slowly with increasing H; (iii) in the paramagnetic phase ($H \gtrsim 70$ kOe), ρ was nearly field independent. Hall measurements showed that the negative magnetoresistance in the canted phase was largely due to an increase in the mobility, and not to an increase in the carrier concentration. At the canted-to-paramagnetic transition, $\partial\rho/\partial H$ and $\partial\rho/\partial T$ changed abruptly. These changes in the derivatives of ρ were used to determine the canted-to-paramagnetic phase boundary $H_c(T)$.

I. INTRODUCTION

The Eu chalcogenides are semiconductors with optical energy gaps in excess of 1 eV. Pure stoichiometric samples of the Eu chalcogenides have very high resistivities at $T \lesssim 300$ K and are, therefore, not very suitable for studies of the electrical transport properties at low temperatures. On the other hand, samples which are nonstoichiometric, or which contain impurities or vacancies, may be reasonably good electrical conductors even at low temperatures. In such samples the coupling between the charge carriers and the spins on the magnetic ions causes the electrical transport properties to be strongly influenced by the state of magnetic order. In the last several years the electrical properties of the Eu chalcogenides have been the subject of several experimental and theoretical studies. These studies have been recently reviewed by Methfessel and Mattis,[1] Haas,[2] von Molnar,[3] and von Molnar and Kasuya.[4] Extensive reference lists may be found in these reviews.

Prior to the present work, electrical transport measurements were largely confined to the ferromagnetic Eu chalcogenides, namely, EuO, EuS, and EuSe. Some of the salient features observed in these materials were (i) A large peak in the resistivity occurred near the ferromagnetic ordering temperature T_c[5-8]; (ii) Hall measurements on doped samples of EuS[6] and EuSe[7] indicated that in these materials the resistivity peak was due largely to a change in the mobility and not to a change in the carrier concentration; (iii) the resistivity peak near T_c was reduced considerably by the application of a magnetic field.[6-8] Negative magnetoresistance was also observed at temperatures several times higher than T_c; (iv) Oliver *et al.*[8] found a large drop in the resistivity of EuO below the Curie temperature, and interpreted their results in terms of a model in which the changes in the resistivity were due largely to a variation in the carrier concentration.

The present paper describes the electrical properties of EuTe single crystals. The dc electrical resistivity and Hall coefficient were studied at $1.5 \leq T \leq 300$ K in magnetic fields up to 140 kOe. Some of the observed phenomena (e.g., large negative magnetoresistance) were similar to those found in the ferromagnetic Eu chalcogenides. However, other phenomena were peculiar to the antiferromagnetic order in EuTe. A few of the preliminary results obtained in the present work were published earlier.[9,10]

The results of the electrical transport measurements are in many cases directly related to the magnetic properties of EuTe. These properties are discussed in the preceding paper[11] (hereafter called I), and in the references which are given here.

II. EXPERIMENTAL TECHNIQUES

A. Samples

Measurements were made on single crystals Nos. 102 and 93 which were grown in the following way.

The compound EuTe was first synthesized by reaction of europium metal with tellurium vapor at 600 °C in sealed quartz ampoules. Crystal No. 102 was grown from the melt directly from this material. The growth took place inside a tungsten crucible which was first sealed near room temperature under a pressure of 1 atm of argon gas, then heated at 2400 °C in a resistance-heated tungsten furnace, and finally cooled at about 5 °C/h. Crystal No. 93 was solution grown by adding 10% europium to the EuTe compound, heating to 2400 °C, and cooling in the same manner as for crystal No. 102.

The melt- and solution-grown crystals had room-temperature resistivities of the order of 10^{-2} Ω cm, and, unlike pure and stoichiometric crystals, were opaque in the red. Semiquantitative analysis for metal impurities showed that a sample from crystal No. 102 contained between 10- and 100-ppm Cu and Mg, and other less-concentrated metallic impurities. The Hall measurements described below showed that both crystals Nos. 102 and 93 were *n* type and that they contained ~10^{19} carriers/cm^3. The source of the charge carriers is unknown. Possible sources are deviations from stoichiometry, foreign impurities (oxygen, for example), or vacancies. The electrical resistivity of samples cut from crystals Nos. 102 and 93 was raised by several orders of magnitude by annealing for 60 h at 1500 °C in an argon atmosphere. All the measurements reported in this paper were carried out on samples which were *not* subjected to this additional annealing procedure.

B. Electrical Measurements

Electrical resistivity and Hall measurements were carried out on rectangular bars with dimensions of $1 \times 1 \times 4$ mm approximately. Four of the six bars had faces parallel to the three equivalent {100} planes. These bars were prepared by cleaving larger specimens. The two remaining bars had (110), (1$\bar{1}$0), and (001) faces, with the [110] direction along the length of each bar. The (001) faces were obtained by cleaving, while the (110) and (1$\bar{1}$0) faces were obtained by lapping. Electrical leads were attached to the cleaved faces of the samples with indium solder using an ultrasonic soldering iron. A typical solder joint had a resistance of a few ohms. When the samples were exposed to air, the solder joints deteriorated after a few days. For this reason, the samples were kept under vacuum, except during the experiments. Under these conditions the solder joints remained unchanged for weeks.

Resistivity measurements were made using a four-terminal arrangement. Such an arrangement was necessary because the resistance of the solder joints was often large compared to the resistance of the sample. The electric current I varied between 1 μA and 10mA. In all cases the resistive voltage V_R was linear with I, and it reversed its sign when the current was reversed. In measuring the magnetoresistance at a fixed temperature, the direction of $\vec{H}$ was reversed at each value of H. The values of V_R for both directions of $\vec{H}$ were always very nearly the same, and they were averaged to obtain the final value.

Because of the finite size of the solder joints, the distance between the voltage leads was not known accurately. As a result, the *absolute* value of the resistivity was subject to a 10–30% uncertainty. However, the *relative* variation of the resistivity with temperature and magnetic field was measured with a precision of ~1%.

Hall measurements were made by reversing the direction of $\vec{H}$ at each value of H. That part of the voltage between the Hall leads which reversed its sign when $\vec{H}$ was reversed was taken to be the Hall voltage. The Hall voltage V_H always reversed its sign when the direction of the current I was reversed. The Hall measurements were made with currents of 1–10 mA. With $I < 1$ mA the Hall voltage was often too small to be measured accurately. The linear dependence of V_H on I was checked in each run at a few values of H.

C. Thermometry

The electrical measurements were made at room temperature, at 77 K with the samples immersed in liquid nitrogen, between 14 and 20 K with the samples immersed in liquid hydrogen, and between 1.6 and 4.2 K with the samples immersed in liquid helium. Vapor-pressure thermometry was used with all the cryogenic liquids.

Resistivity measurements were also performed between 4.2 and 14 K. In these measurements the sample was mounted on a copper block which was situated in an evacuated copper can. The copper can was surrounded by liquid helium. The temperature of the copper block was regulated by a heater and was measured with a carbon resistance thermometer whose magnetoresistance had been determined previously.[12] Thermal contact between the sample, the copper block, and the thermometer was improved by using Crycon grease.[13] Near 10 K the accuracy of the temperature measurements in the copper can was ±0.2 K.

In other experiments the resistivity at $H = 0$ was measured from 20 to 300 K. These measurements were carried out in the evacuated copper can described in the preceding paragraph, but a calibrated platinum resistance thermometer was used instead of a carbon resistance thermometer.

D. Magnetic Fields

High magnetic fields, up to 140 kOe, were pro-

TABLE I. Physical properties of the various samples. Here $\rho_T \equiv \rho(0, T)$ is the zero-field resistivity at temperature T, R_T is the Hall coefficient at temperature T, μ_T is the Hall mobility at temperature T, n is the carrier concentration deduced from the Hall coefficient at 77 K, and T_N is the Néel temperature. The absolute values of ρ and μ are uncertain to within 10–30%. The uncertainty in the Hall coefficient is 2%, and the uncertainty in T_N is 0.2 K.

	Sample No.					
	93	102a	102b	102c	102d	102e
Current direction	[100]	[100]	[100]	[110]	[100]	[110]
ρ_{300} (Ω cm)	0.012	0.004	0.024	0.018	0.010	0.02
R_{300} (cm^3/C)	−0.53	•••	−0.80	−0.97	−0.53	−1.16
μ_{300} (cm^2/V sec)	44	•••	33	54	51	58
ρ_{77} (Ω cm)	0.008	0.003	0.021	0.017	0.008	0.02
R_{77} (cm^3/C)	−0.52	•••	−0.78	−0.95	−0.49	−1.12
$n \equiv \frac{1}{\lvert R_{77} e \rvert}$ (cm^{-3})	1.2×10^{19}	•••	8.0×10^{18}	6.6×10^{18}	1.3×10^{19}	5.6×10^{18}
$\rho_{4.2}$ (Ω cm)	0.7	0.25	7	7	0.8	8
T_N (K)	9.7	9.7	9.6	•••	9.8	•••

duced in Bitter-type solenoids. The external (applied) magnetic field H_{ext} was known to an accuracy of 0.5%. To obtain the internal magnetic field H_{int} inside the sample, it was necessary to estimate the demagnetizing field H_d and subtract it from H_{ext}. In estimating H_d, the shape of the sample was approximated by that of an ellipsoid of revolution, and use was made of the magnetization curves obtained in I. At low temperatures, H_d amounted to several percent of H_{ext}. The uncertainty in the final value of H_{int} was ±2%.

III. EXPERIMENTAL RESULTS

Measurements were performed on five samples which were cut from single crystal No. 102, and on one sample which was cut from single crystal No. 93. Some of the important electrical characteristics of these samples are listed in Table I. The absolute accuracy in the values of the resistivities (and hence the mobilities) in this table are subject to a 10–30% uncertainty, as explained in Sec. IIB. The accuracy in the relative change of the resistivity of a given sample with temperature is much higher. Note that the five samples which were cut from crystal No. 102 had significantly different resistivities and carrier concentrations. However, the qualitative behavior of the resistivity and the Hall coefficient as a function of H and T was similar in all these samples.

A. Resistivity

The dependence of the resistivity $\rho(H, T)$ on H and T was investigated at $1.6 \leq T \leq 300$ K and $0 \leq H_{ext} \leq 100$ kOe. The results at zero field and at finite fields are described separately.

1. *Resistivity at* $H = 0$

Figure 1 shows the zero-field resistivity $\rho(0, T)$ as a function of T for two samples. As T decreased, $\rho(0, T)$ first decreased near room temperature, then went through a shallow minimum, and finally increased rapidly at low temperatures. Note that (a) the temperature where $\rho(0, T)$ had a minimum was substantially higher than the Néel temperature $T_N \cong 9.6$ K of these two samples, and (b) at temperature $T \lesssim 2T_N$, the increase of $\rho(0, T)$ with decreasing T became very rapid. Another interesting feature is that at T_N, the derivative $\lvert \partial\rho(0, T)/\partial T \rvert$ changed abruptly from a higher value in the paramagnetic phase to a lower value in the antiferromagnetic phase. This is shown more clearly in Fig. 2 where $\rho(0, T)$ is plotted vs $1/T$ for temperatures near T_N. For sample No. 102b, $\rho(0, T)$ actually went through a small local maximum near T_N, although this maximum is not easily discernible in Fig. 2. The transition temperature T_N was determined from the change in $\partial\rho/\partial T$. The justification of this procedure of determining T_N lies in the fact that it leads to results which agree with magnetization and ultrasonic data.[11,14] The values of T_N obtained from the change in $\partial\rho/\partial T$ were subject to an uncertainty of ~0.2 K, and are given in Table I.

At 4.2 K, the zero-field resistivity of all the samples was 80–400 times larger than at 77 K. Between 4.2 and 1.6 K, $\rho(0, T)$ increased exponentially with $1/T$, i.e., $\rho(0, T) \sim e^{\Delta/T}$. The value for Δ varied from sample to sample. For sample No. 102a, for example, $\Delta \cong 11$ K, while for sample No. 102d, $\Delta \cong 14$ K.

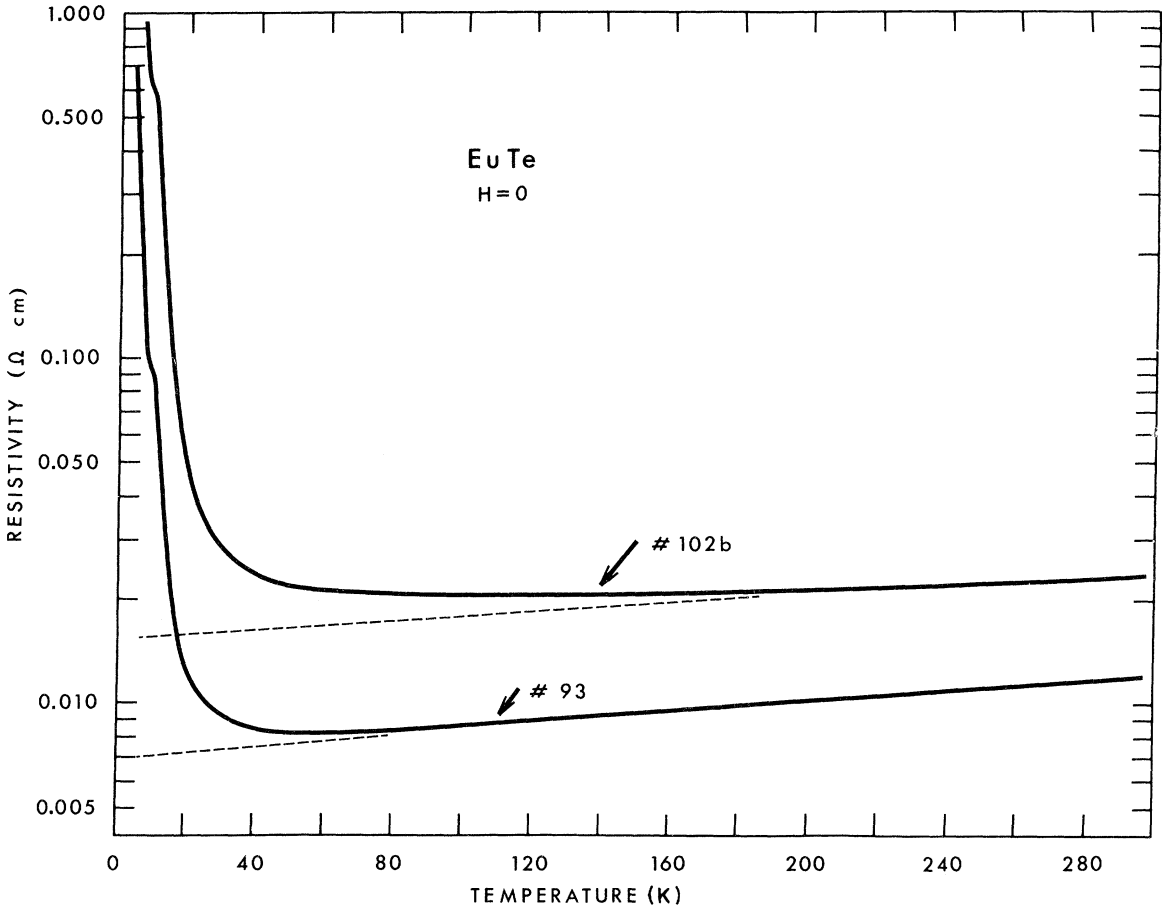

FIG. 1. Temperature variation of the zero-field resistivity $\rho(0, T)$ for samples Nos. 93 and 102b. The dashed lines represent (approximately) the extrapolations of the high-temperature data to low temperatures.

2. *Resistivity at* $H > 0$

Measurements of $\rho(H, T)$ in finite magnetic fields were made by (i) measuring ρ as a function of T at a fixed H, and (ii) measuring ρ as a function of H at a fixed T. The first type of measurement was performed only on samples Nos. 93 and 102a, at $2 \leq T \leq 14$ K and with the measuring current $\vec{I}$ along $\vec{H}$. The results for both samples were similar. Some of the results for sample No.102a are shown in Fig. 3. Note that a large negative magnetoresistance existed both at $T > T_N$ and at $T < T_N$. Note also that the order-disorder transition (from the paramagnetic phase to the antiferromagnetic phase $H \lesssim 10^3$ Oe, and from the paramagnetic phase to the canted phase at $H \gtrsim 10^3$ Oe), was accompanied by a change in $\partial\rho/\partial T$. As the sample entered the ordered phase (antiferromagnetic or canted), $|\partial\rho/\partial T|$ decreased for $0 \leq H \leq 20$ kOe, but increased for $H \geq 30$ kOe. The two types of behavior are illustrated in Fig. 3 by the curve for $H = 0$, and by the curve for $H = 39$ kOe. At fields above ~74 kOe the samples were in the paramagnetic phase at all temperatures, [11] and $\rho(H, T)$ was a smooth function of T, with no discontinuities in $\partial\rho/\partial T$. This behavior is illustrated in Fig. 3 by the curve for $H = 84$ kOe.

Measurements of $\rho(H, T)$ as a function of H at constant T were performed on several samples at various temperatures. At room temperature, the transverse resistivity ($\vec{I} \perp \vec{H}$) was measured in samples Nos. 93 and 102d. The resistivity was field independent in the range 0–100 kOe, to within an accuracy of 2%.

Magnetoresistance measurements at 77 K were performed on samples Nos. 93, 102c, and 102d. The transverse magnetoresistance of these three samples is shown in Fig. 4. Note that in an increasing field, ρ first increased, then reached a maximum, and finally decreased at high fields. The parallel magnetoresistance ($\vec{I} \parallel \vec{H}$) in sample No. 102d was also measured at 77 K in fields up to 100 kOe, and the results were very close to those obtained for the transverse magnetoresistance in this sample.

Measurements of the magnetoresistance at liquid-

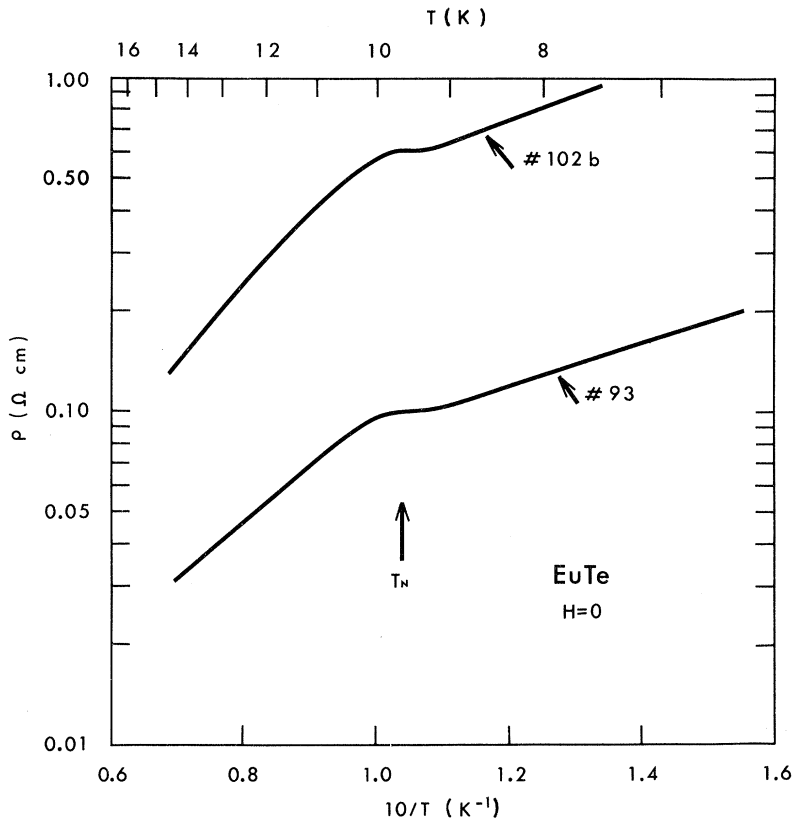

FIG. 2. Temperature variation of the zero-field resistivity $\rho(0, T)$ for samples Nos. 93 and 102b at temperatures near T_N. Note that the lower abscissa scale is for $10/T$ while the upper abscissa scale is for T.

hydrogen temperatures were carried out on sample No. 102d. The results at 14.5 K for the transverse magnetoresistance ($\vec{I} \parallel [100]$, $\vec{H}[010]$) are shown in Fig. 5. At 100 kOe the resistivity of this sample was about $\frac{1}{3}$ of its value at $H = 0$. Note that the negative magnetoresistance had a tendency to saturate at high fields, although complete saturation was not achieved at 100 kOe. In the same sample the magnetization at $T = 14.5$ K and $H = 100$ kOe was equal to 0.74 of its saturation value. At 100 kOe, $\rho \cong 7 \times 10^{-3}$ Ω cm, which was slightly lower than the zero-field resistivity at 77 K. This result agrees with that found in sample No. 102a (see the curve for $H = 84$ kOe in Fig. 3). It is noteworthy that at 14.5 K a field of 1 kOe hardly changed the resistivity. This situation should be contrasted with the results at liquid-helium temperatures, which are presented next.

The H dependence of ρ at $T \leq 4.2$ K can be divided into three different parts corresponding to three field ranges. The first range is from 0–~1 kOe, where ρ decreased very rapidly with increasing H. This behavior is illustrated by the results in Fig. 6 which were obtained at 4.2 K. At this temperature the ratio $\rho(1\text{ kOe})/\rho(0)$ was of order 0.1 for all samples. As T decreased, $\rho(0)$ increased as $e^{\Delta/T}$ while $\rho(1\text{ kOe})$ increased much more slowly. As a result, the negative magnetoresistance in the range 0–1 kOe became larger at lower temperatures. At 1.7 K, $\rho(1\text{ kOe})/\rho(0)$ was of order 10^{-3}. Magnetization measurements showed that at liquid-helium temperatures the magnetization of samples Nos. 102 and 93 increased rapidly with H in the range 0–1 kOe.[11]

The second field range, from ~1 kOe to H_c, corresponds to the canted phase. A large negative magnetoresistance was observed in this range but $|\partial\rho/\partial H|$ was considerably smaller than in the range 0–1 kOe. As T decreased, $\rho(1\text{ kOe})$ increased slowly while $\rho(H_c)$ remained approximately unchanged. Thus the magnitude of the negative magnetoresistance in the canted phase increased slightly with decreasing T.

The third field range, for fields above H_c, corresponds to the paramagnetic phase. In this range ρ was almost H independent. Also, for any fixed field well above H_c, ρ was approximately temperature independent at $T < 4.2$ K. These observations are probably related to the fact that at $T \leq 4.2$ K, the magnetization at any fixed field above H_c was nearly saturated. The behavior of $\rho(H)$ in both the canted and paramagnetic phases is illustrated by the results in Fig. 7. Note that at H_c the derivative $\partial\rho/\partial H$ decreased abruptly. This abrupt change in $\partial\rho/\partial H$ is shown more clearly in Fig. 2 of Ref. 9.

The dependence of ρ on the relative orientation

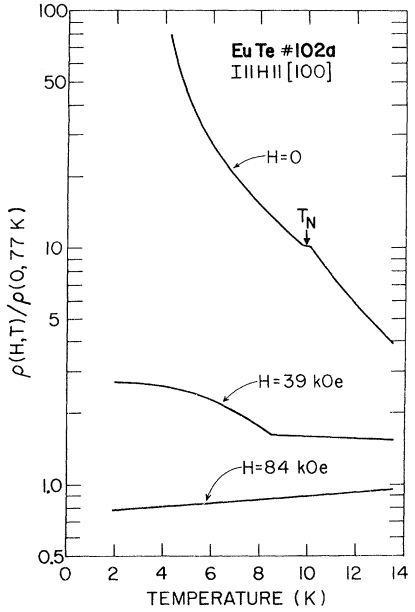

FIG. 3. Temperature variation of the resistivity of sample No. 102a at several values of the magnetic field. The resistivity was normalized to $\rho(0, 77\ \mathrm{K})$.

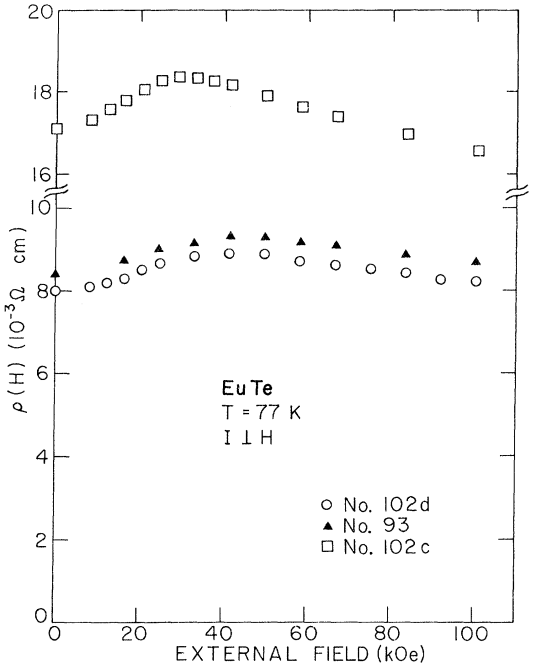

FIG. 4. Transverse magnetoresistance of samples Nos. 93, 102c, and 102d at 77 K. Note the break in the ordinate scale.

between $\vec{I}$ and $\vec{H}$ was measured at 4.2 K in samples Nos. 102c and 102d. The results for sample No. 102d are shown in Fig. 7. The open circles in this figure correspond to the transverse resistivity ($\vec{I}\parallel[100], \vec{H}\parallel[010]$), whereas the solid triangles correspond to the parallel resistivity $\vec{I}\parallel\vec{H}\parallel[100]$. It is apparent that the results for ρ vs H_{int} were very nearly the same in both cases. The measurements in sample No. 102c were carried out with (a) $\vec{I}\parallel\vec{H}[110]$, (b) $\vec{I}\parallel[110], \vec{H}\parallel[1\bar{1}0]$, and (c) $\vec{I}\parallel[110], \vec{H}\parallel[001]$. The results for ρ vs H_{int} were very nearly the same in all three cases. From the discontinuity in $\partial\rho/\partial H$, the transition field H_c was determined for all three field directions. The value for H_c for $\vec{H}\parallel[001]$ did not differ by more than 2 kOe from the value for $\vec{H}\parallel[110]$ or $\vec{H}\parallel[1\bar{1}0]$.

The transition between the canted phase and the paramagnetic phase was marked by discontinuties in $\partial\rho/\partial T$ and $\partial\rho/\partial H$. Thus the temperature variation of the transition field $H_c(T)$ could be determined from the resistivity data. The same phase boundary was determined more accurately from differential magnetization measurements,[11] and from ultrasonic measurements.[14] Figure 8 shows the canted-to-paramagnetic phase boundary as determined from the resistivity measurements (experimental points) and from the ultrasonic measurements (solid curve).

B. Hall Effect

In nonmagnetic materials the Hall voltage V_H is given by

$$V_H = R H_{\mathrm{ext}}(I/t), \tag{1}$$

where t is the thickness of the sample along H_{ext} and R is the Hall coefficient. In a one-band model the concentration n of charge carriers is given approximately by $n = |1/Re|$. In magnetic materials V_H is often expressed as

$$V_H = (R_0 H_{\mathrm{int}} + R_1^* M)(I/t), \tag{2}$$

where M is the magnetization.[6,15] Equation (2) can

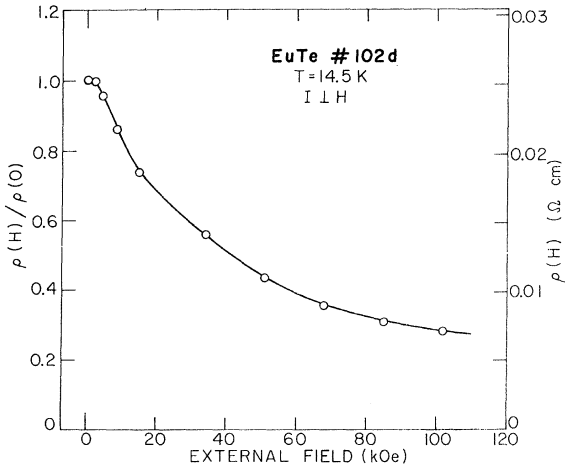

FIG. 5. Transverse magnetoresistance of sample No. 102d at 14.5 K. Note the position of the zero on the abscissa scale.

be also written as

$$V_H = (R_0 B + R_1 M)(I/t), \tag{3}$$

where B is the magnetic induction inside the sample, and

$$R_1 = R_1^* - 4\pi R_0. \tag{4}$$

Authors who use Eq. (2) call R_0 the normal (or ordinary) Hall coefficient, and R_1^* the anomalous (or extraordinary) Hall coefficient. Those who use Eq. (3) call R_0 the normal Hall coefficient and R_1 the anomalous Hall coefficient.[2] The normal Hall coefficient is related approximately to n as $n = |1/R_0 e|$.

It will be shown below that for EuTe at $T \ll T_N$ and for $H > H_c$, the term $R_1 M$ in Eq. (3) is very small compared to $R_0 B$. Guided by this fact, it will be assumed that $R_1 M \ll R_0 B$ at all temperatures and magnetic fields. With this assumption Eq. (3) may be written as

$$V_H = R_0 B(I/t). \tag{5}$$

In analyzing the Hall data at $T \gg T_N$ we shall use Eq. (1) to obtain R. Since in this temperature range B is very nearly equal to H_{ext}, the coefficient R obtained from Eq. (1) will be close to the coefficient R_0 which one would have obtained by using Eq. (5). At $T \lesssim T_N$, however, the difference between B and H_{ext} amounts to several percent, and we shall use Eq. (5) to calculate R_0.

At 300 and 77 K the Hall voltage was linear with the applied magnetic field. This is illustrated in Fig. 9 by the data for sample No. 102d at 77 K. The results for the Hall coefficient obtained from such data are given in Table I. Note that the Hall coefficient was negative, indicating that the electrical conduction was predominately due to electrons.

Measurements of the Hall voltage at liquid-hydrogen temperatures were confined to sample No. 102d. The magnetic field variation of V_H and of R at 14.5 K is shown in Fig. 10.[16] Note that $|R|$ decreased slowly as H_{ext} increased. However, this decrease of $|R|$ was very small compared with the decrease of ρ with increasing magnetic field, in the same sample and under the same conditions (see Fig. 5). Thus $R(8.5\text{ kOe}) = 1.2R(102\text{ kOe})$, whereas $\rho(8.5\text{ kOe}) = 3.1\ \rho(102\text{ kOe})$. The most obvious interpretation of these results is that the negative magnetoresistance at 14.5 K was largely due to an increase in the mobility, and not to an increase in the carrier concentration.

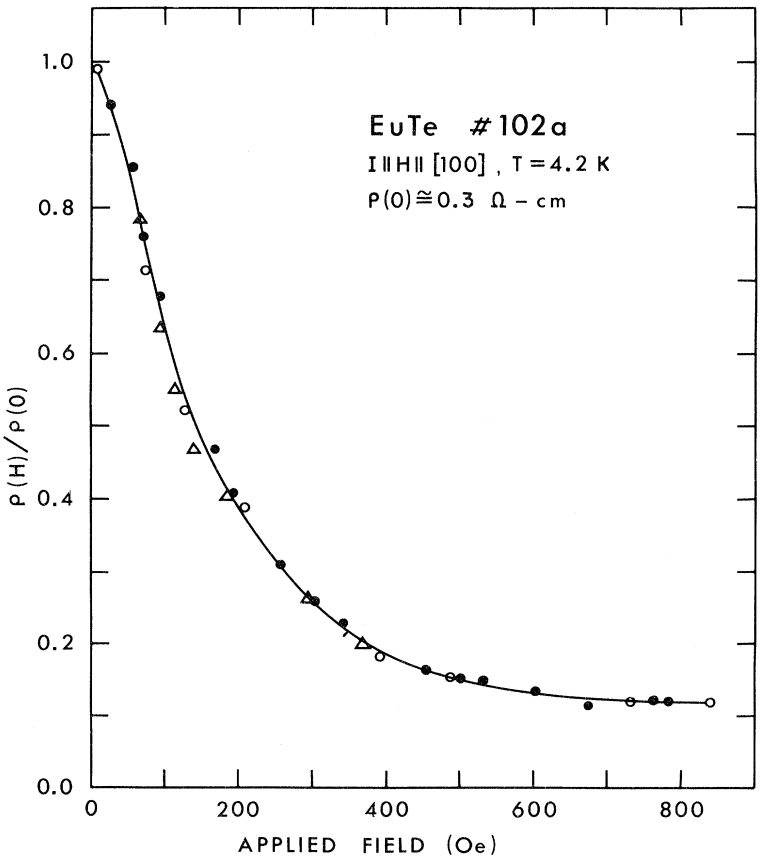

FIG. 6. Magnetic field variation of the resistivity of sample No. 102a at $T = 4.2$ K. Only the low-field data are shown here.

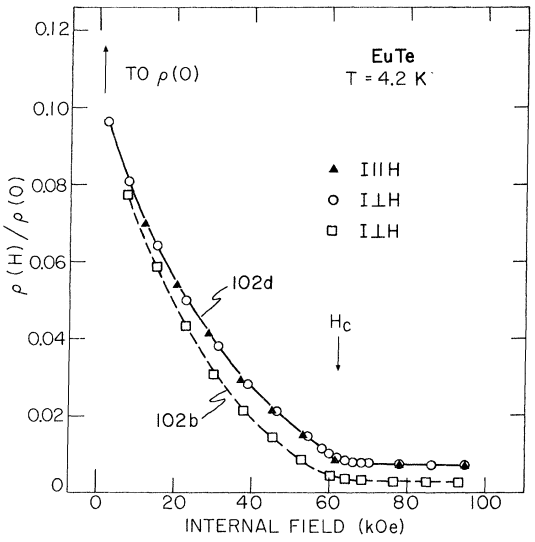

FIG. 7. Magnetic field variation of the resistivity of samples Nos. 102b and 102d at 4.2 K. The large drop in the resistivity at fields of $\sim 10^2$ Oe is not shown. Note the position of the zero on the abscissa scale. Note also that for sample No. 102d the results with $\vec{I} \parallel \vec{H}$ are very nearly the same as those with $\vec{I} \perp \vec{H}$.

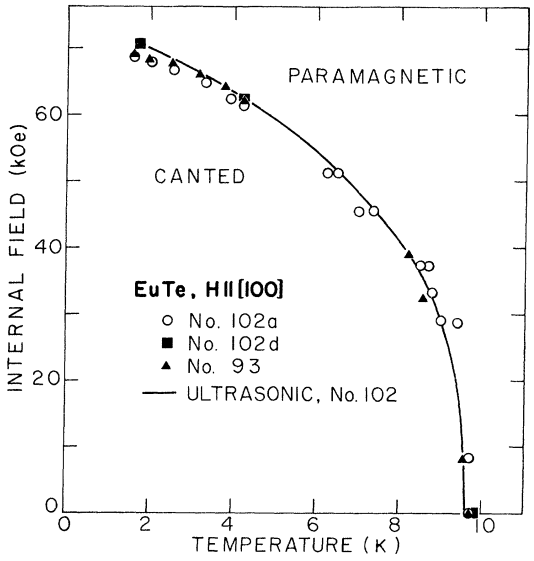

FIG. 8. The boundary $H_c(T)$ between the paramagnetic and the canted phases as determined from resistivity measurements (experimental points) and from ultrasonic measurements (solid curve).

Hall measurements at $T < T_N$ were carried out at 4.2 and at 1.6 K. Figure 9 shows the Hall voltage V_H at 4.2 K as a function of H_{ext} for sample No. 102d. At $H > H_c$, V_H was linear with H_{ext}, but at $H < H_c$ deviations from linearity appeared. The same qualitative behavior was exhibited by sample No. 102d at 1.6 K, and by sample No. 102b at 4.2 K.

The Hall data for sample No. 102d at 1.6 K were analyzed for the purpose of determining the relative magnitudes of the normal and anomalous Hall coefficients. While both R_0 and R_1 may depend on magnetic field, it was assumed that above 90 kG, where the magnetization was saturated,[11] both R_0 and R_1 were field independent. With this assumption Eq. (3) predicts a linear dependence of V_H on B at $B > 90$ kG, since the term $R_1 M$ is a constant. This prediction was borne out experimentally. A least-squares fit of the data above 90 kG to Eq. (3) indicated that at these fields $R_1 M / R_0 B \lesssim 0.03$. Thus at high fields, the anomalous term in the Hall voltage was very small compared to the normal term, so that V_H was well approximated by Eq. (5). The same best fit gave $R_0 = -0.48$ cm^3/C for sample No. 102d at 1.6 K, which is very close to the value for R at 77 K (see Table I).

Guided by the analysis of the high-field data at 1.6 K, it was assumed that $R_1 M \ll R_0 B$ at all temperatures and magnetic fields. The Hall data at 4.2 and 1.6 K were then compared with Eq. (5). Figure 11 shows the variation of R_0 with H_{int} for samples Nos. 102b and 102d at 4.2 K, and for sample No. 102d at 1.6 K. Comparison of the results at 4.2 K with the resistivity data which are shown in Fig. 7 indicates that the variation of R_0 with H_{int} was much smaller than the variation of ρ. Thus, for sample No. 102d at 4.2 K, $R_0(25\text{ kOe}) = 1.4\, R_0(100\text{ kOe})$, whereas $\rho(25\text{ kOe}) = 6.8\rho(100\text{ kOe})$. For sample No. 102b at 4.2 K, $R_0(25\text{ kOe}) = 1.6\, R_0(100\text{ kOe})$, whereas $\rho(25\text{ kOe}) = 15\rho(100\text{ kOe})$. These

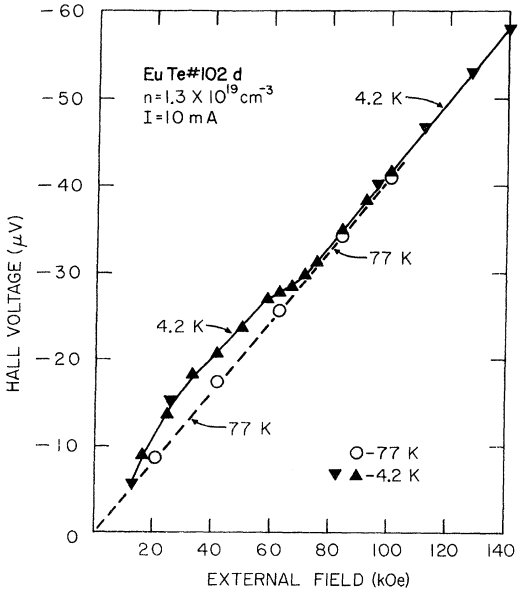

FIG. 9. Magnetic field variation of the Hall voltage in sample No. 102d at 77 and 4.2 K.

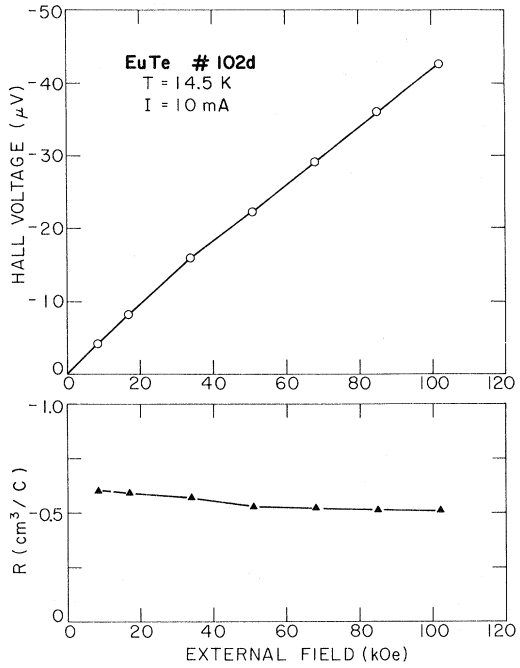

FIG. 10. Magnetic field variation of the Hall voltage V_H and the Hall coefficient R for sample No. 102d at 14.5 K. The Hall coefficient was calculated from Eq. (1) (see Ref. 16).

results seem to indicate that the large negative magnetoresistance which occurs *in the canted phase* at 4.2 K is due largely to an increase in the mobility and not to an increase in the carrier concentration. The same conclusion holds also at 1.6 K.

The Hall measurements at liquid-helium temperatures were limited to fields above ~20 kOe. At lower fields the resistive voltage, due to the unintentional offset of the Hall leads, was large and prevented accurate measurements of V_H. In particular, no Hall measurements were carried out at fields below 1 kOe. Therefore, we cannot say whether the large negative magnetoresistance at fields of order 10^2 Oe (see Fig. 6) was due to a change in the mobility or to a change in the carrier concentration.

IV. DISCUSSION

In the Eu chalcogenides there is a large exchange interaction between the charge carriers and the spins of the magnetic ions. This s-f exchange interaction causes the magnetic properties to depend on the presence of charge carriers, and leads to a dependence of the electrical transport properties on the state of magnetic order. The effects of charge carriers on the magnetic properties of EuTe have been described in I. Here we are concerned with the effects of the s-f interaction on the electrical transport properties of EuTe.

The theory of the electrical transport properties of magnetic semiconductors was reviewed by several authors.[1-4] However, it is important to realize at the outset that the available theoretical results for the electrical transport properties in *antiferromagnetic semiconductors* are not sufficiently detailed, or sufficiently quantitative, to give a reasonably complete interpretation of the various aspects of the present data. The discussion and conclusions below are therefore qualitative, and incomplete in some respects.

Consider Fig. 1. At temperatures far above T_N electrical conduction in the EuTe samples appears to be band conduction with mobilities of about 50 cm^2/V sec. Near room temperature $\rho(0, T)$ decreases with decreasing T, presumably because the scattering of electrons by phonons decreases. At much lower temperatures, but well above T_N, $\rho(0, T)$ starts to increase with decreasing T. This leads to a resistivity minimum. At temperatures $T \lesssim 2T_N$, $\rho(0, T)$ increases rapidly with decreasing T.

The large increase of $\rho(0, T)$ at low temperatures appears to be due to the interaction of the charge carriers with the magnetic ions. The strongest evidence for this conclusion comes from the large negative magnetoresistance (see Figs. 3 and 5–7). The negative magnetoresistance in the liquid-helium range, and also at 14.5 K, approaches saturation at high fields where the magnetization approaches saturation. The saturation value of ρ at high fields is approximately equal to the value obtained by ex-

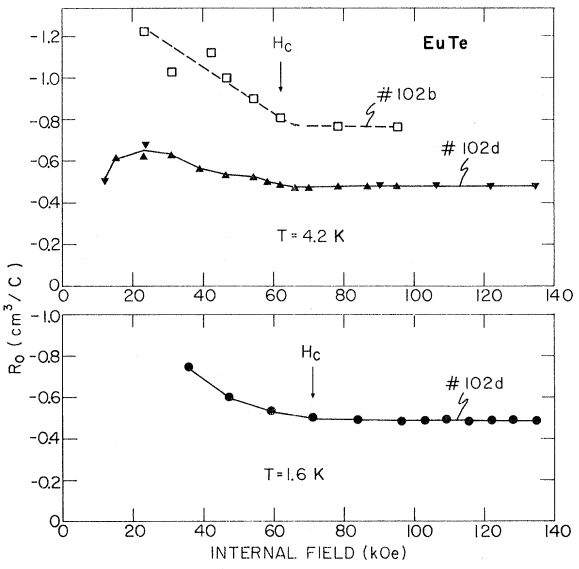

FIG. 11. Normal Hall coefficient R_0 as a function of H_{int} for samples Nos. 102b and 102d at 4.2 K, and for sample No. 102d at 1.6 K. R_0 was calculated from Eq. (5).

trapolating the high-temperature portion of the $\rho(0, T)$ vs T curve to low temperatures (see dashed lines in Fig. 1).[17] Thus the entire increase of $\rho(0, T)$ at low temperatures is removed by a large magnetic field.

Further evidence for the coupling between the magnetic ions and the conduction electrons is the existence of discontinuities in $\partial\rho/\partial H$ and $\partial\rho/\partial T$ at the boundary between the ordered phase (antiferromagnetic or canted) and the paramagnetic phase (see Figs. 2, 3, and 7). These discontinuities show that a change in the magnetic order affects the motion of the charge carriers.

One theoretical idea which may be of particular relevance to the present work is that of "self-trapping" of the charge carriers by the double-exchange interaction. The self-trapping mechanism is reviewed in Sec. 71 of Ref. 1. The basic idea of self-trapping is as follows. Because of the double-exchange interaction, an electron will cause the spins in an antiferromagnet to be canted relative to each other (see Ref. 11, Sec. II B). If the electron is free to move through the lattice then it will cant all the spins uniformly throughout the lattice. A second possibility is that the electron will be localized and cause a large canting of the spins around itself, but a small canting of spins far away from itself. It turns out that for low carrier concentrations the double-exchange interaction favors large local-spin distortions by localized electrons over small uniform-spin distortions by free electrons. Thus it is energetically favorable for the electrons to become localized, or trapped. In the presence of an electric field, the localized electrons (and their local-spin distortions) are able to move through the lattice, but only slowly. The motion of self-trapped carriers in the antiferromagnetic phase was recently considered by Kasuya.[18] The mechanism of self-trapping may be responsible for the high values of ρ at low temperatures and at zero, or low, magnetic fields.

The Hall measurements at 14.5 K indicate that the large negative magnetoresistance at this temperature is almost entirely due to an increase in the mobility and not to an increase in the number of charge carriers. Similarly, at 4.2 and 1.6 K the large negative magnetoresistance in the canted phase is almost entirely due to an increase in the mobility. The low mobility at low fields and at low temperatures may be accounted for by Kasuya's model for the antiferromagnetic polaron.[18] In high fields, the resistivity approaches a constant low value. This may be explained by the fact that at high fields the spins on the magnetic ions all point in the same direction, and therefore have the periodicity of the lattice. In this case scattering due to the magnetic ions is not expected. Also, the self-trapping mechanism is not expected when all the spins are parallel to each other.

In the liquid-helium range there is a large drop in the resistivity at fields of $\sim 10^2$ Oe. This is also the field range where the magnetization of the samples increases rapidly with H, presumably because the weak ferromagnetic moment which results from the canting of the spins is aligned.[11] It is unfortunate that no Hall data could be obtained at these low fields so that we cannot say whether the drop in the resistivity is due to a change in the mobility or to a change in the carrier concentration.

At 77 K the magnetoresistance exhibits an unusual H dependence (see Fig. 4). This behavior may be the result of two competing mechanisms: one which causes the positive magnetoresistance at low fields, and another which causes the negative magnetoresistance at high fields. The origin of the first mechanism is not known. The second mechanism may be the same one which dominates the magnetoresistance at lower temperatures.

It is clear from the preceding discussion that much work remains to be done before the electrical transport properties of EuTe are understood in detail. On the experimental side, studies of EuTe doped with different known amounts of various impurities should be made. However, the greater need is for a theory with workable models which reproduce the salient features of the data.

ACKNOWLEDGMENTS

The authors wish to thank V. Diorio for technical assistance, and in particular for making the electrical connections to the samples. We also wish to thank R. E. Fahey for assisting in the growth of the EuTe single crystals, and Dr. A. J. Strauss for useful comments.

---

*Visiting scientist at the Francis Bitter National Magnet Laboratory on leave from the University of São Paulo, S. Paulo, Brazil, C.P. 8105.

†Supported by Conselho Nacional de Pesquisas, Brazil, and the Ford Foundation.

‡Supported by the U. S. Air Force Office of Scientific Research.

§Operated with support from the U. S. Air Force.

[1]S. Methfessel and D. C. Mattis, in *Handbuch der Physik*, edited by S. Flügge (Springer-Verlag, Berlin, 1968), Vol. 18, Part 1.

[2]C. Haas, CRC Crit. Rev. Solid State Sci. 1, 47 (1970).

[3]S. von Molnar, IBM J. Res. Develop. 14, 269 (1970).

[4]S. von Molnar and T. Kasuya, *Proceedings of the Tenth International Conference on the Physics of Semiconductors, Boston*, 1970 (U.S. Atomic Energy Commission, Oak Ridge, Tenn., 1970), p. 233.

[5]R. R. Heikes and C. W. Chen, Physics 1, 159 (1964).

[6]S. von Molnar and T. Kasuya, Phys. Rev. Letters 21, 1757 (1968).

[7]S. von Molnar and S. Methfessel, J. Appl. Phys. 38,

959 (1967).
[8]M. R. Oliver, J. O. Dimmock, and T. B. Reed, IBM J. Res. Develop. 14, 276 (1970); M. R. Oliver, J. A. Kafalas, J. O. Dimmock, and T. B. Reed, Phys. Rev. Letters 24, 1064 (1970); see also G. Petrich, S. von Molnar, and T. Penney, *ibid.* 26, 885 (1971).
[9]Y. Shapira, S. Foner, and N. F. Oliveira, Jr., Phys. Letters 32A, 323 (1970).
[10]Y. Shapira, S. Foner, and N. F. Oliveira, Jr., Phys. Letters 33A, 323 (1970).
[11]N. F. Oliveira, Jr., S. Foner, Y. Shapira, and T. B. Reed, preceding paper, Phys. Rev. B 5, 2634 (1972) (hereafter called I).
[12]L. J. Neuringer and Y. Shapira, Rev. Sci. Instr. 40, 1314 (1969).
[13]Manufactured by Air Products and Chemicals, Allentown, Penn.
[14]Y. Shapira and T. B. Reed, following paper, Phys. Rev. B 5, 2657 (1972).
[15]E. M. Pugh and N. Rostoker, Rev. Mod. Phys. 25, 153 (1953).
[16]At 14.5 K the difference between H_{ext} and B in this sample was ~5%. Hence the coefficient R calculated from Eq. (1) was ~5% higher than the coefficient R_0 calculated from Eq. (5).
[17]The saturation value of ρ at high fields and at low temperatures may even be lower than the value obtained by extrapolating the high-temperature data for $\rho(0, T)$ to low temperatures. This is not surprising since even at high temperatures $\rho(0, T)$ is expected to contain a small magnetic contribution.
[18]T. Kasuya, Solid State Commun. 8, 1635 (1970).

PHYSICAL REVIEW B VOLUME 5, NUMBER 7 1 APRIL 1972

EuTe. III. Ultrasonic Behavior

Y. Shapira
Francis Bitter National Magnet Laboratory, Massachusetts Institute of Technology, Cambridge, Massachusetts* 02139

and

T. B. Reed
Lincoln Laboratory,† Massachusetts Institute of Technology, Lexington, Massachusetts 02173
(Received 7 June 1971)

Ultrasonic attenuation and velocity measurements were carried out on EuTe single crystals at $1.4 \leq T \leq 14$ K and in magnetic fields up to 100 kOe. At $H = 0$, the attenuation for shear waves with $\vec{q} \parallel [100]$ increased abruptly as the sample entered the antiferromagnetic phase at $T_N = (9.6 \pm 0.2)$ K. At $T < T_N$ the attenuation of some modes of propagation was higher in the canted phase than in the paramagnetic phase. The canted-to-paramagnetic transition was accompanied by an abrupt decrease and/or by a sharp peak in the attenuation of some modes of propagation. The canted-to-paramagnetic transition field $H_c(T)$ was determined as a function of temperature. At $1.4 \leq T \leq 4.2$ K, $H_c(T)$ followed the theoretical $T^{3/2}$ law. At $T = 0$, $H_c(0) \cong 74$ kOe, which leads to an intersublattice exchange field $H_E(0) \cong 37$ kOe. At liquid-helium temperatures, large changes in the ultrasonic attenuation and velocity occurred in fields of order 10^2 Oe. The elastic constants at 77.6 K, in cgs units, are $c_{11} = (9.36 \pm 0.4) \times 10^{11}$, $c_{44} = (1.63 \pm 0.07) \times 10^{11}$, and $c_{12} = (0.67 \pm 0.6) \times 10^{11}$. These lead to an adiabatic compressibility $\kappa_s = (2.8 \pm 0.4) \times 10^{-12}$ cgs units, and to a Debye temperature $\Theta = 189$ K.

I. INTRODUCTION

In the preceding two papers[1,2] (hereafter called I and II) the physical properties of EuTe were reviewed with special emphasis on the magnetic and electrical transport characteristics. The present paper describes the ultrasonic behavior of EuTe at low temperatures and in magnetic fields up to 100 kOe. In particular, the ultrasonic behavior near the canted-to-paramagnetic transition is described in detail. Earlier work on the ultrasonic behavior of antiferromagnets at high magnetic fields is reviewed in Ref. 3. In this reference the ultrasonic behavior near the magnetic phase transitions of MnF_2, FeF_2, CoF_2, Cr_2O_3, α-Fe_2O_3, and Cr is summarized. With the exception of Cr, all these materials are uniaxial antiferromagnets in which the axis of symmetry is the preferred direction for the spins at $T = 0$. The present study in the easy-plane cubic antiferromagnet EuTe uncovered several new features which were not observed previously in other antiferromagnets. Many of these new features remain unexplained. Also included in this paper are results for the elastic constants from which the Debye temperature and compressibility are deduced.

A significant portion of the present work is devoted to the determination of the boundary, in the H-T plane, between the canted and the paramagnetic phases.[4] While the magnetic phase diagrams of several antiferromagnets have been studied in the past, there have been only a few experimental